Heliyon 10 (2024) e30110

Contents lists available at ScienceDirect

Heliyon

journal homepage: www.cell.com/heliyon

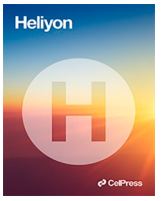

Research article

OSTF1 knockdown mitigates IL-1β-induced chondrocyte injury via inhibiting the NF-κB signaling pathway

Bin Hu [a], Gongwen Du [b,*]

[a] Department of Hand and Foot Surgery, Yijishan Hospital of Wannan Medical College, No. 2, Zheshan West Road, Wuhu, Anhui, China
[b] Department of Orthopaedics, The First Affiliated Hospital of Anhui Medical University, No. 218, Jixi Road, Hefei, Anhui, China

ARTICLE INFO

Keywords:
Osteoarthritis
OSTF1
NF-κB signaling pathway
IL-1β
Chondrocyte
Apoptosis
Inflammation
Extracellular matrix degradation

ABSTRACT

Osteoarthritis (OA) is an age-related joint disease characterized by progressive heterogeneous changes in articular cartilage and subchondral bone. Osteoclast stimulating factor 1 (OSTF1) is a small intracellular protein involved in bone formation and bone resorption. However, to our best knowledge, its role in OA is still unclear. In this study, an OA rat model was established by anterior cruciate ligament transection (ALCT). OSTF1 was increased in the cartilage tissues of OA patients and OA rats. Next, the role of OSTF1 in interleukin-1β (IL-1β)-induced chondrocyte apoptosis, inflammation and extracellular matrix degradation was explored through loss of function assays. Strikingly, OSTF1 knockdown relieved IL-1β-induced chondrocyte apoptosis, with decreased cleaved caspase-3 and cleaved PARP levels. Besides, OSTF1 knockdown restrained IL-1β-induced inflammation and degradation of extracellular matrix of chondrocytes. Subsequently, the molecular mechanism of OSTF1 was explored. Transcriptomic analysis revealed the potential gene network map regulated by OSTF1 knockdown. Some differentially expressed genes (DEGs) were involved in regulating the NF-κB signaling pathway. Furthermore, our results demonstrated that OSTF1 knockdown inhibited IL-1β-activated the NF-κB signaling pathway. Ultimately, we analyzed the potential gene network map regulated by OSTF1 and its downstream NF-κB. Bioinformatics analysis showed that 18 DEGs in OSTF1-silenced chondrocytes overlapped with the NF-κB downstream targets. Collectively, our findings indicate that OSTF1 knockdown mitigates IL-1β-induced chondrocyte injury via inhibiting the NF-κB signaling pathway.

1. Introduction

Osteoarthritis (OA) is a slow, progressive and degenerative disease that is the most common and expensive form of arthritis [1]. The incidence of OA increases in prevalence with age and is a major musculoskeletal cause of mobility impairment in older adults [2]. The most frequently affected sites of OA are the hands, knees, hips and spine [3]. Its major clinical symptoms include chronic pain, joint instability, stiffness, joint deformities and radiographic joint space narrowing [4,5]. The current primary treatments are low-impact

Abbreviations: OA, osteoarthritis; IL-1β, interleukin-1β; ALCT, anterior cruciate ligament transection; qRT-PCR, quantitative real-time PCR; TNF-α, tumor necrosis factor-α; OSTF1, Osteoclast stimulating factor 1; H&E, Hematoxylin and eosin; DEGs, differentially expressed genes; ANOVA, one-way analysis of variance; OASRI, osteoarthritis research society international; NAFLD, non-alcoholic fatty liver disease; PARP, poly ADP-ribose polymerase.

* Corresponding author.
E-mail address: dugongwen1987@163.com (G. Du).

https://doi.org/10.1016/j.heliyon.2024.e30110
Received 26 February 2024; Received in revised form 18 April 2024; Accepted 19 April 2024
Available online 20 April 2024

aerobic exercise [6], weight loss [7], acupuncture [8] and surgery [9]. Currently, except for total joint replacement surgery, there are no effective interventions to slow the process of OA or delay the irreversible degeneration of cartilage [1]. Thus, it is urgently necessary to reveal the pathogenesis of OA.

Articular cartilage mainly consists of tissue fluid, type II collagen and proteoglycans [10]. Articular chondrocytes, the only cell type in articular cartilage, are applied for generating and maintaining the cartilaginous extracellular environment [11]. Furthermore, collagen and proteoglycans form the hydrated structure of the matrix which provides tensile and elastic strength to the articular cartilage, allows the joint to maintain a proper biomechanical function [2]. Accumulating evidence suggests that chondrocytes in OA patients produce a large number of proinflammatory cytokines, which cause chondrocyte apoptosis and cellular matrix degradation, resulting in severe cartilage degeneration [12,13]. It seems that relieving cartilage destruction may benefit the treatment of OA.

Osteoclast stimulating factor 1 (OSTF1), a protein containing the SH3 domain, was originally thought to be a factor involved in indirect osteoclast activation [14]. Previous study has revealed that OSTF1 indirectly enhances osteoclast formation and bone-resorption activity in cell culture assays through the supernatant of transfected 293 cells [15]. Our previous showed that OSTF1 was greatly upregulated in cartilage tissues of OA patients. However, any role for OSTF in the development of OA has not been explored.

Interleukin-1β (IL-1β) and tumor necrosis factor-α (TNF-α) seem prominent and of major importance to cartilage destruction [16, 17]. In addition, these inflammatory factors can combine with receptors on the articular cartilage surface to activate the NF-κB pathway in chondrocytes [18]. NF-κB signaling pathway plays a crucial role in inflammatory response, which may contribute to chondrocyte cell death and cartilage destruction [19]. However, whether OSTF1 affects OA process by regulating the NF-κB signaling pathway needs further verification.

Herein, we explored the role of OSTF1 in OA as well as the underlying mechanism. Uncovering the role of OSTF1 in OA may contribute to the OA therapy.

2. Materials and methods

2.1. Human OA cartilage samples

Cartilage tissues were collected from patients with OA who underwent total knee joint replacement surgery. Tissues were not fibrous or wholly degenerated, and subchondral bone was not included. Undamaged areas were sampled as normal cartilage in patients above. Ethical approval was obtained from the Medical Research Ethics Committee of the First Affiliated Hospital of Anhui Medical University, and clinical study was conducted in accordance with the Declaration of Helsinki. Written informed consent was obtained from each participant.

2.2. Establishment of OA rat model

Animal experiments were approved by the Medical Research Ethics Committee of Anhui Medical University and carried out in accordance with the "Guide for the Care and Use of Laboratory Animals". SD rats were randomly divided to the sham group or OA group. ALCT was performed in 12-week-old male rats (300–400 g) to induce right knee OA [20]. Briefly, after induction of anesthesia, the right knees of rats were disinfected and a 2 cm parapatellar skin incision was made on the medial side of the joint. The patella was dislocated and the anterior cruciate ligament was transected. The sham group underwent intra-articular anesthesia and surgical incision without ACLT. For the time-course experiment, rats were sacrificed at 2, 4 and 8 weeks postoperatively, and tissues were collected from the right knee joints for further experiments.

2.3. Hematoxylin and eosin (H&E) staining

Rat cartilage tissues were embedded in paraffin blocks which were cut to a thickness of 5 μm. Sections were then dewaxed in xylene and hydrated by ethanol. Finally, sections were stained with hematoxylin (Solarbio, Beijing, China) for 5 min and eosin for 3 min. Photographing was made with a DP73 microscope (Olympus, Tokyo, Japan).

2.4. Safranin O staining and histological scoring

Sections were deparaffinized in xylene and rehydrated by ethanol. Then sections were stained with safranin O (Solarbio) for 2 min, and images were photographed under a microscope. Histological scoring was conducted in accordance with the Osteoarthritis Research Society International (OARSI) grading system [21]. The score was determined in multiple serial sections from each murine knee.

2.5. Immunohistochemical analysis

For immunohistochemical analysis, sections were incubated with 3 % H_2O_2 at room temperature for 15 min to eliminate endogenous peroxidase activity. Primary OSTF1 antibody (1:1000, 10671-1-AP, ThermoFisher, Pittsburgh, USA) was incubated at 4 °C overnight, and followed by incubation with secondary goat anti-rabbit IgG-HRP (ThermoFisher) for 1 h at 37 °C. The positive staining was visualized using DAB (MXB® Biotechnology, Fuzhou, China). Cell nuclei were stained with hematoxylin, and images were

observed under a microscope.

2.6. Construction of adenovirus vector

The shRNA targeting OSTF1 (ACTAAAGATATTTGCATGTCGCTATGTGTTCT GGGAAATCACCATAAACGTGAAATGTCTTTGGATTTGGGAATCTTATAAGTTCTGTATGAGACCACTCGGTGGAAAGGAA-CATGCAAAGTTCAAGAGACTTTGCATGTTCCTTTCCACCTTTTT) or negative control sequence was inserted into pShuttle-CMV vector (Fenghui Biotechnology, Changsha, China), respectively. Then the recombinant plasmid was transferred to HEK293T cells, generating OSTF1-shRNA adenovirus.

2.7. Cell culture and IL-1β treatment

Rat cartilage tissues were collected carefully and treated with 3 mg/ml (0.25 %) collagenase II (Biosharp, Hefei, China) for 2 h at 37 °C. Next, the digested chondrocytes were cultured in DMEM/F12 medium (Procell, Wuhan, China) with 10 % FBS (Tianhang Biotechnology, Zhejiang, China) at 37 °C and 5 % CO_2. For infection, cells were cultured overnight and infected with adenovirus. After 24 h of infection, cells were treated with 10 ng/ml IL-1β.

2.8. CCK-8 assay

CCK-8 reagent (Beyotime, Shanghai, China) was added into the cells and incubated for 2 h. Finally, the supernatant was collected, and absorbance of the colored solution was quantified at 450 nm on a microplate reader (Biotek, Winooski, USA).

2.9. TUNEL staining

Cells were treated with 0.1 % Triton X-100 (Beyotime). Then 200 μl TUNEL reaction solution was added to cells and cells were incubated at 37 °C for 1 h in the dark. Cell nuclei were stained with DAPI (Aladdin, Shanghai, China) for 5 min. Images were captured under a microscope.

2.10. Quantitative real-time PCR (qRT-PCR) analysis

Total RNA was extracted and reverse transcribed into cDNA by BeyoRT II M-MLV reverse transcriptase (Beyotime). cDNA was subjected to qRT-PCR using SYBR green Kit (Solarbio, Beijing, China). The constructed PCR reaction system was put into ExicyclerTM96 (BIONEER, Daejon, Korea). The relative gene expression values were calculated using the $2^{-\Delta\Delta Ct}$ method. GAPDH was used as internal control. The primers are listed in Table 1.

2.11. Western blotting assay

Cells were lysed in RIPA buffer (PMSF = 1 mmol/l, Solarbio), and proteins were isolated. Then protein concentration was measured using a BCA protein concentration Assay Kit (Beyotime). The proteins were separated by 10 % SDS-PAGE (20 μg protein in each lane, Solarbio) and transferred to PVDF membranes (Millipore, Billerica, MA, USA). OSTF1 (1:1000, 10671-1-AP, Proteintech, Wuhan, China), cl-caspase 3 (1:1000, AF7022, Affinity, Changzhou, China), cl-PARP (1:1000, AF7023, Affinity), aggrecan (1:1000, DF7561, Affinity), collagen-II (1:1000, AF0135, Affinity), MMP1 (1:1000, A22080, Abclonal, Wuhan, China), MMP13 (1:1000, AF5355, Affinity), p-p65 (1:1000, AF2006, Affinity) and p65 (1:1000, AF5006, Affinity) primary antibodies were added and incubated overnight at 4 °C, followed by incubation with the respective secondary antibodies (1:3000) at 37 °C for 1 h. ECL reagent (Solarbio) was used for

Table 1
qRT-PCR primers.

Name	Sequence (5′-3′)
OSTF1 forward	TTTACTCAGCCGAATGTG
OSTF1 reverse	TCTTCTTCAGGAGCGATG
TNF-α forward	CGGAAAGCATGATCCGAGAT
TNF-α reverse	AGACAGAAGAGCGTGGTGGC
IL-6 forward	CAGCCACTGCCTTCCCTA
IL-6 reverse	TTGCCATTGCACAACTCTTT
aggrecan forward	CGCCCATCATCAGAAACC
aggrecan reverse	TCCAGGCAGCGTAGAGC
collagen-II forward	AGAGCGGAGACTACTGGATTG
collagen-II reverse	TCTGGACGTTAGCGGTGTT
MMP1 forward	AAAGGCAGGTTCTACATTCGT
MMP1 reverse	CTAACTTCATAAGCAGCATCA
MMP13 forward	GCCAGAACTTCCCAACCA
MMP13 reverse	ACCCTCCATAATGTCATACCC

luminescence detection, and data quantification was utilized by Gel-Pro-Analyzer software.

2.12. Immunofluorescence staining

After cells were fixed in 4 % paraformaldehyde, 0.1 % Triton X-100 was added to cells, followed by 1 % BSA (Sangong Biotech, Shanghai, China). Then cells were incubated at room temperature for 15 min, 30 min and 15 min, respectively. Primary antibodies (Collagen II, 1:200, AF5006, Affinity or P65, 1:200, AF0135, Affinity) were added and incubated overnight at 4 °C, followed by incubation with goat anti-rabbit IgG-Cy3 (1:200, A27039, Invitrogen, Carlsbad, USA) at room temperature for 1 h. Cell nuclei were stained with DAPI. Then images were captured by a microscope.

2.13. RNA sequencing

Chondrocytes were infected with adenovirus for 24 h, and then treated with IL-1β (10 ng/ml) for 24 h. Chondrocytes were then harvested for RNA sequencing. RNA extraction was performed with the TRIzol (Invitrogen). RNA integrity was then checked by Bioanalyzer 2100 (Agilent, Santa Clara, USA). The captured mRNA was fragmented using the Magnesium Fragmentation Kit (NEBNext® Magnesium RNA Fragmentation Module, Ipswich, USA), and the fragmented RNA was subjected to reverse transcriptase (SuperScript™ II Reverse Transcriptase, Invitrogen) to synthesize cDNA. Finally, PCR amplification was performed and the products were purified to obtain the final library. We performed paired-end sequencing using an Illumina Novaseq™ 6000 (LC Bio Technology, Hangzhou, China) following standard procedures.

For the bioinformatics analysis, firstly, the raw data was filtered, including removing junctions, repetitive sequences and low-quality sequences. Aligned the sequencing data to the genome. Genes or transcripts were assembled and quantified with FPKM. Differentially expressed genes (DEGs, $|\log2\text{-fold change}|>1$) between samples were analyzed, and P value < 0.05 was considered as differentially expressed. In addition, GO and KEGG pathway enrichment analyses were performed.

2.14. Statistical analysis

Data were expressed as mean ± SD. Student's t-test was used to compare the data between two groups. Comparison between groups was performed using one-way analysis of variance (ANOVA), followed by the Bonferroni post-hoc test. P value < 0.05 was considered to be statistically significant.

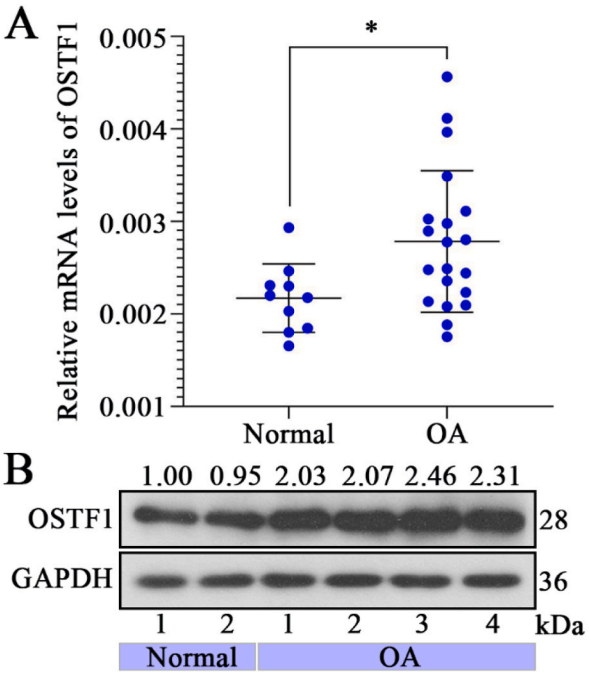

Fig. 1. The expression of OSTF1 is upregulated in cartilage tissues of OA patients. (A) The mRNA levels of OSTF1 in cartilage tissues of OA patients (n = 20) and healthy volunteers (n = 10). (B) The protein levels of OSTF1 in cartilage tissues of OA patients (n = 4) and healthy volunteers (n = 2). (*p < 0.05).

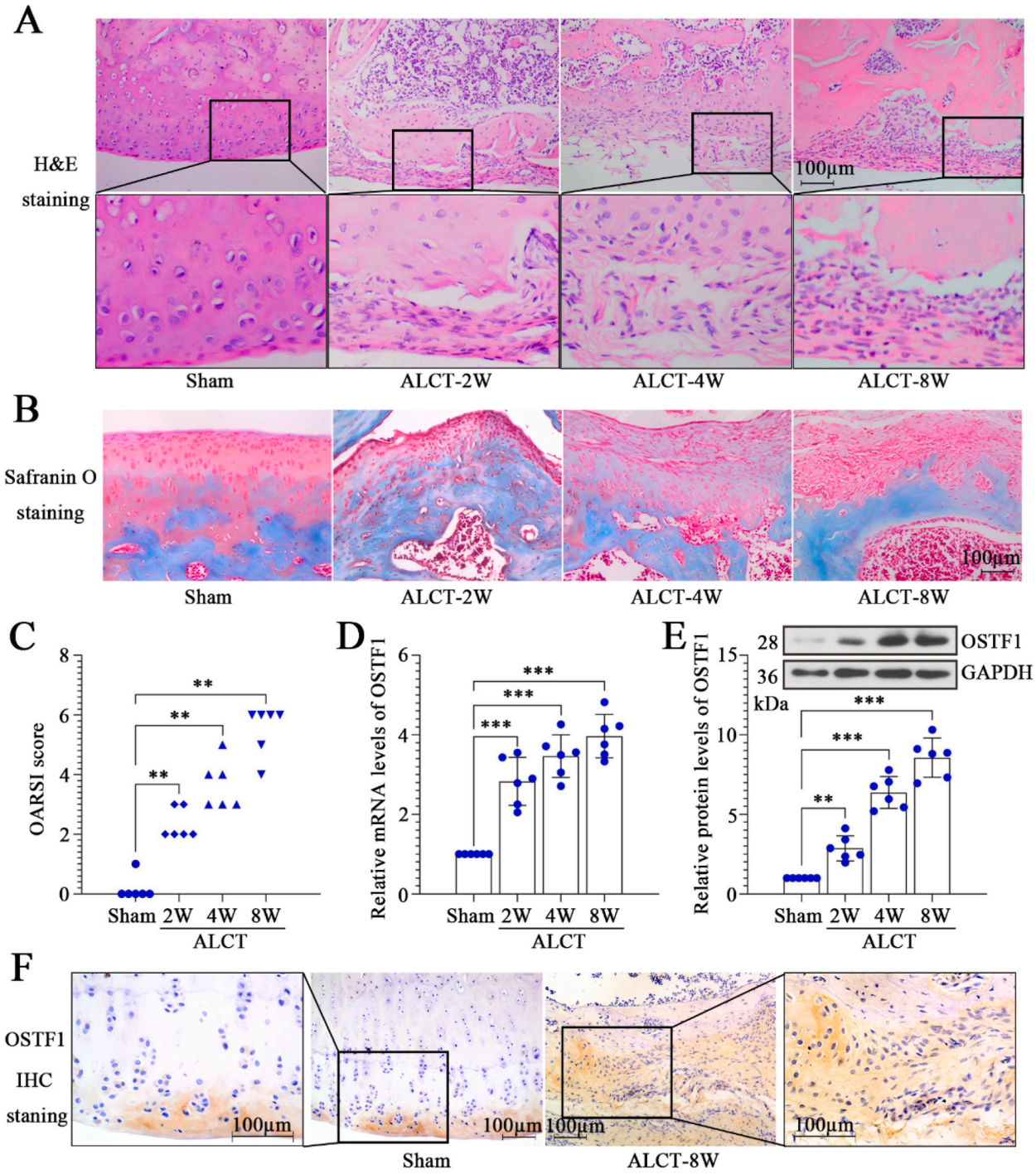

Fig. 2. The expression of OSTF1 is increased in the knee cartilage tissues of OA rats. OA was induced by ALCT surgery in rats. (A) H&E staining showed the pathological changes in cartilage tissues at 2, 4 and 8 weeks after surgery (the scale bar represented 100 μm). (B) The safranin O staining exhibited the proteoglycan in cartilage tissues (the scale bar represented 100 μm). (C) The OASRI scores of rat knee cartilage. (D–E) The mRNA and protein levels of OSTF1 in knee cartilage tissues of rats were determined by qRT-PCR and western blotting. (F) The OSTF1 expression was detected by immunohistochemistry staining (the scale bar represented 100 μm). n = 6. (**p < 0.01, ***p < 0.001).

3. Results

3.1. The expression of OSTF1 is upregulated in cartilage tissues of OA patients

To ascertain the change of OSTF1 levels in the development of OA, the expression of OSTF1 in cartilage tissues of normal and OA patients was examined using qRT-PCR and western blotting. The clinical results revealed that the mRNA and protein expression levels of OSTF1 in cartilage tissues of OA patients were significantly upregulated relative to the normal (Fig. 1A–B). These data presented that OSTF1 was highly expressed in cartilage tissues of OA patients.

3.2. The expression of OSTF1 is increased in the knee cartilage tissues of OA rats

We first established an animal model of OA using the ALCT method. Next, we assessed the damage of knee articular cartilage in ALCT-operated rats. H&E staining showed that the joint morphology of the sham group was normal, whereas the cartilage surface of OA rats exhibited damage, defects and structural breakage with a decreased number of chondrocytes (Fig. 2A). By Safranin O staining, we observed the erosion and hypocellularity of articular cartilage and the loss of proteoglycan in the ALCT group (Fig. 2B). The results of OASRI scores were consistent with the histological analysis (Fig. 2C). In addition, we verified the expression pattern of OSTF1 in cartilage tissues of OA rats. Similarly, our data showed that after the surgery, the mRNA and protein levels of OSTF1 were significantly upregulated in the OA group relative to the sham rats (Fig. 2D–E). With the progression of OA, the expression of OSTF1 was gradually increased and reached the highest at the 8th week (Fig. 2D–E). Strikingly, the above results were observed in immunohistochemistry staining assay (Fig. 2F). Overall, these findings suggested that OSTF1 was increased in the knee cartilage tissues of OA rats, and it may be involved in the progression of OA.

3.3. Knockdown of OSTF1 in chondrocytes is mediated by adenoviral vector

To verify the effects of OSTF1 knockdown on OA process, we constructed an adenoviral vector carrying shRNA targeting OSTF1 and

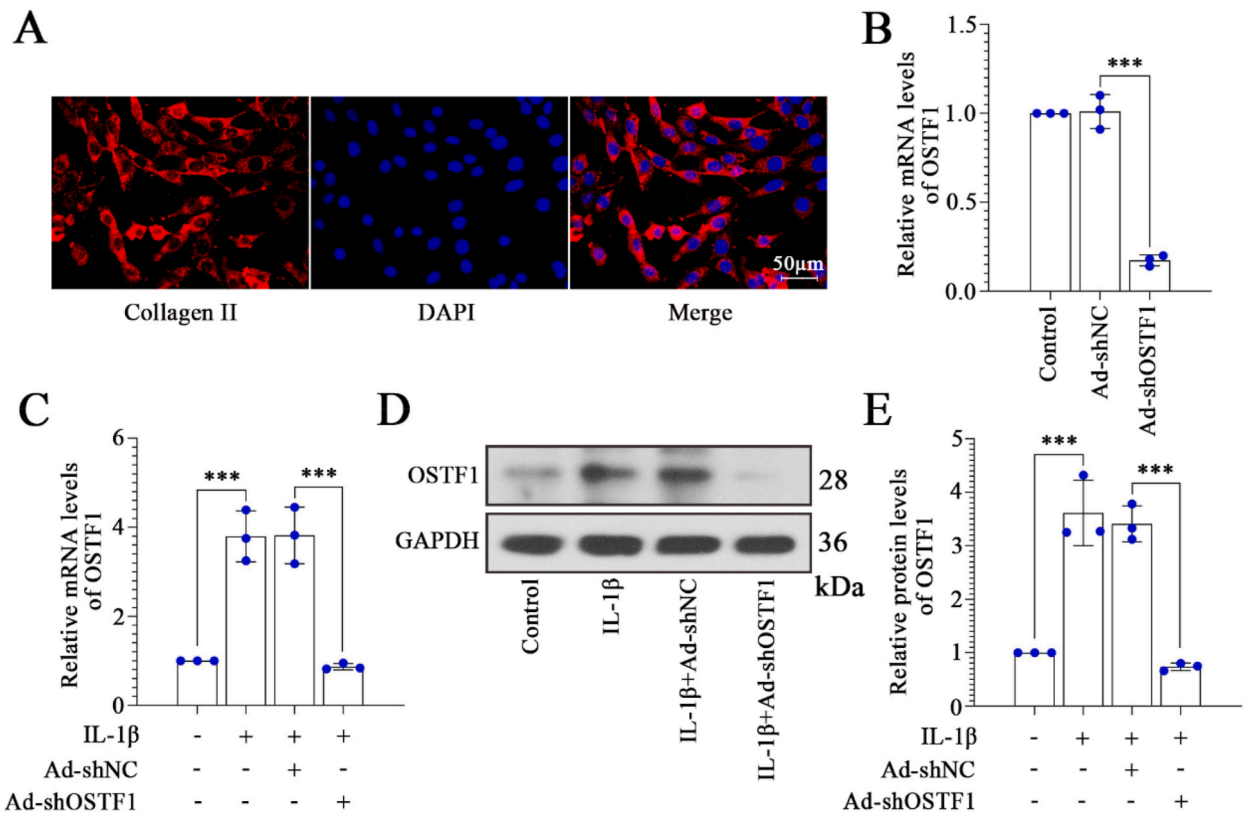

Fig. 3. The knockdown of OSTF1 in chondrocytes is mediated by adenoviral vector. (A) The primary chondrocytes were isolated from knee cartilage tissue of rats, and identified by immunofluorescent staining of collagen II (the scale bar represented 50 μm). (B) The knockdown fragment of OSTF1 was cloned into adenovirus vector, and the rat chondrocytes were infected with this adenovirus (Ad-shOSTF1). The knockdown efficiency was confirmed by qRT-PCR. (C–E) The mRNA and protein levels of OSTF1 were detected by qRT-PCR and western blotting in chondrocytes with IL-1β stimulation and infection of Ad-shOSTF1 or Ad-shNC. n = 3. (***$p < 0.001$).

detected the expression of OSTF1 in chondrocytes. Firstly, chondrocytes were identified by immunofluorescence staining for type II collagen, and the results indicated that chondrocytes had typical morphologies of chondrocytes, such as spherical, fusiform and slab-stone shape (Fig. 3A). Next, we examined the knockdown efficiency of OSTF1 in chondrocytes, as shown in Fig. 3B. Moreover, IL-1β-treated chondrocytes were used as the cellular model of OA. As displayed, the mRNA and protein expression levels of OSTF1 were significantly upregulated by IL-1β administration, which was abolished by OSTF1 knockdown (Fig. 3C–E). Taken together, the above results indicated that the levels of OSTF1 were elevated in the IL-1β-mediated cell model.

3.4. *OSTF1 knockdown relieves IL-1β-induced apoptosis and inflammation in chondrocytes*

We further addressed the effects of OSTF1 knockdown on IL-1β-induced chondrocyte injury. CCK-8 data displayed that IL-1β decreased chondrocyte viability, while OSTF1 knockdown reversed the effects of IL-1β on cell viability (Fig. 4A). Moreover, TUNEL staining results showed that IL-1β greatly increased TUNEL-positive chondrocytes, which was abolished by OSTF1 knockdown (Fig. 4B), thus reducing cell apoptosis. In addition, western blotting results confirmed that IL-1β led to the upregulation of cleaved caspase-3 and cleaved PARP, whereas, the levels of these two proteins were markedly downregulated due to OSTF1 knockdown

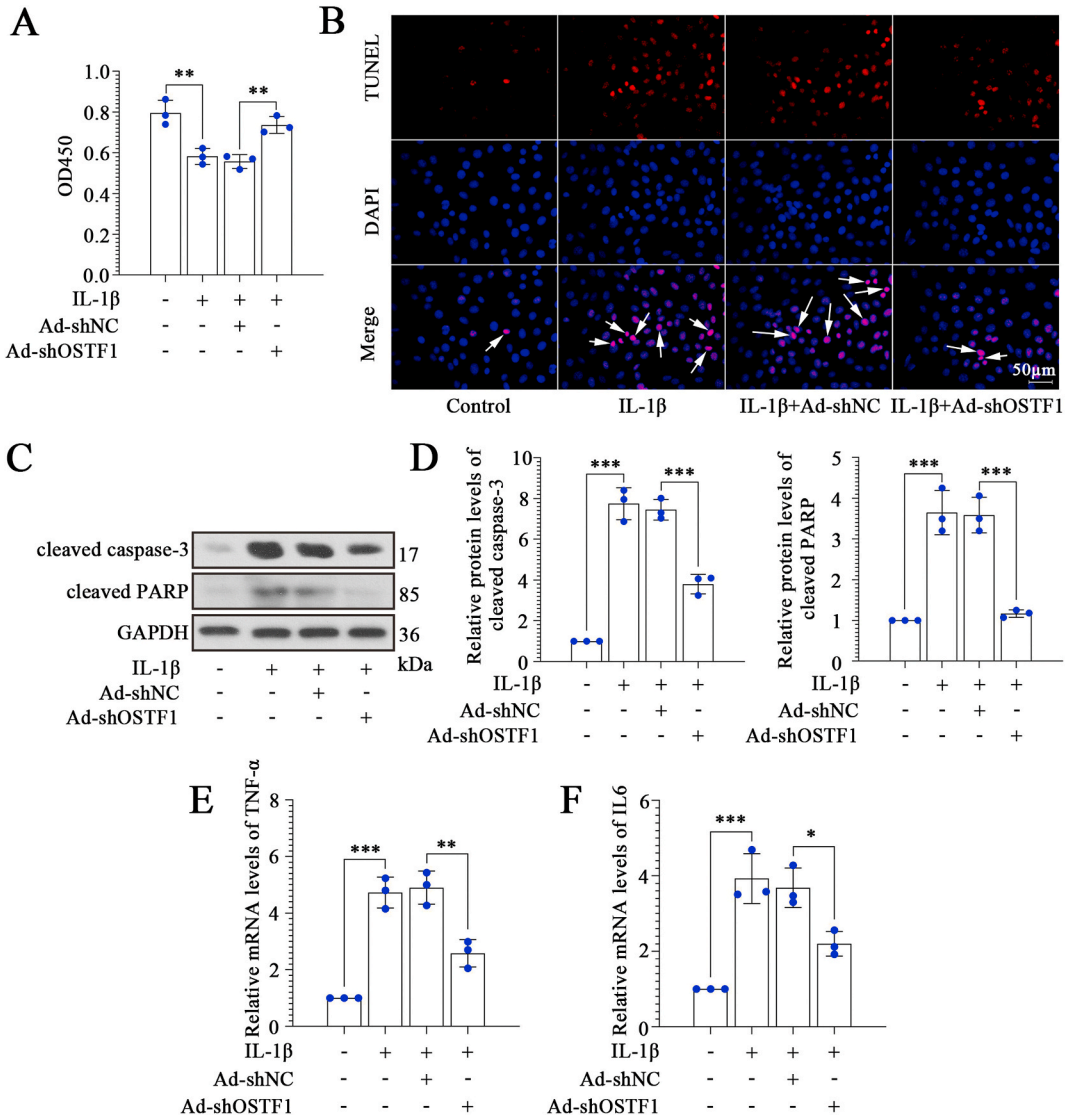

Fig. 4. OSTF1 knockdown relieves IL-1β-induced apoptosis and inflammation in chondrocytes. (A) The viability of chondrocytes was determined by CCK-8 assay after IL-1β administration and OSTF1 knockdown. (B) TUNEL was used to display the apoptotic cells (the arrows indicated TUNEL-positive cells, and the scale bar represented 50 μm). (C–D) The levels of cleaved caspase-3 and cleaved PARP in IL-1β-stimulated and OSTF1-silenced chondrocytes. (E–F) The mRNA levels of inflammatory factors TNF-α and IL-6 were determined by qRT-PCR. n = 3. (*$p < 0.05$, **$p < 0.01$, ***$p < 0.001$).

(Fig. 4C–D).

We also identified the effects of OSTF1 on IL-1β-induced inflammation. qRT-PCR results showed that OSTF1 knockdown largely decreased the mRNA expression of pro-inflammatory cytokines TNF-α and IL-6 (Fig. 4E–F), further abolishing the effects of IL-1β on proinflammatory cytokine levels. Thus, these data demonstrated that OSTF1 knockdown largely increased chondrocyte viability and relieved apoptosis and inflammation, which further reversed the effects of IL-1β on chondrocyte injury in the development of OA.

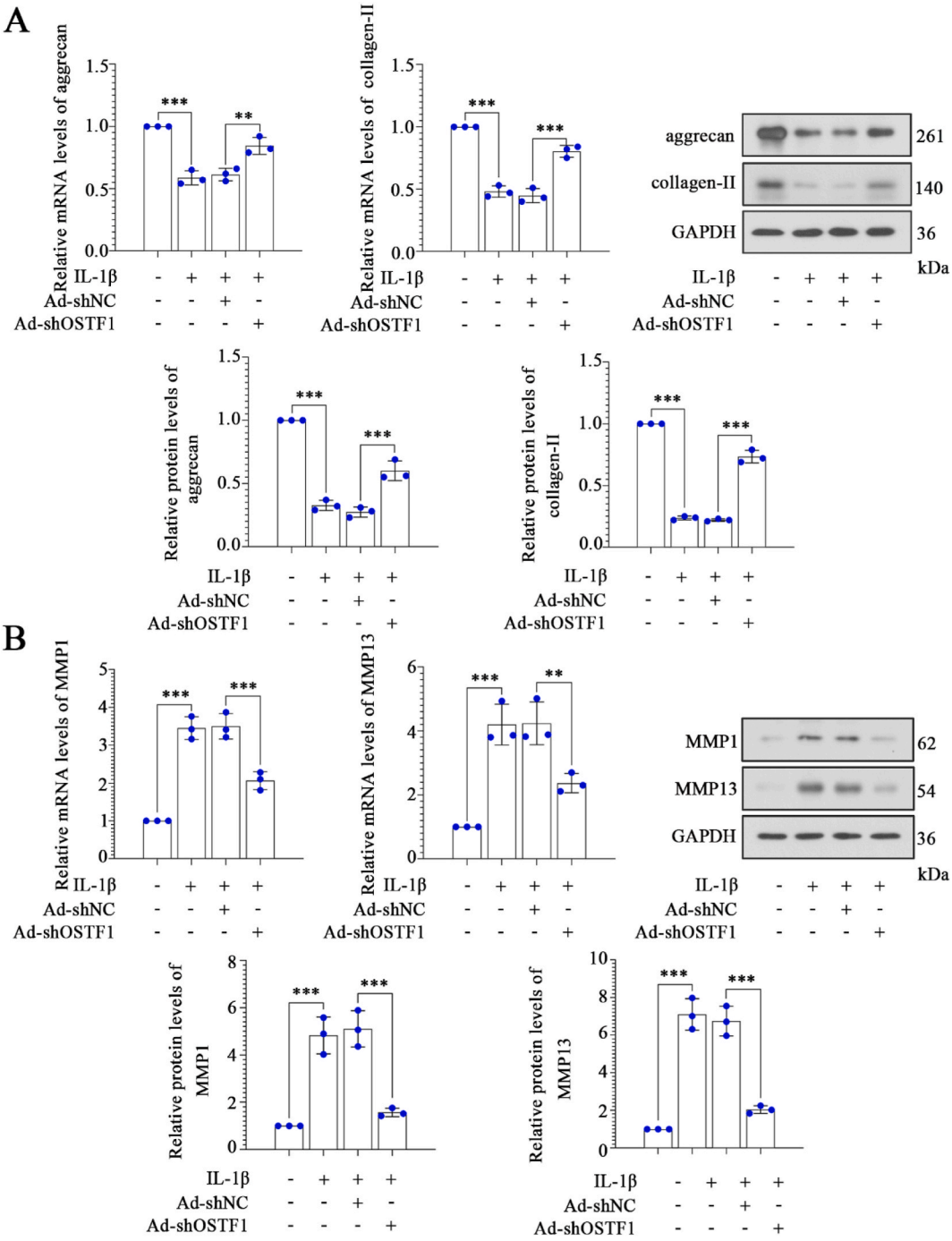

Fig. 5. OSTF1 knockdown inhibits IL-1β-induced the extracellular matrix degradation of chondrocytes. (A–B) The expressions of collagen II, aggrecan, MMP1 and MMP13 in chondrocytes were detected by qRT-PCR and western blotting. n = 3. (**p < 0.01, ***p < 0.001).

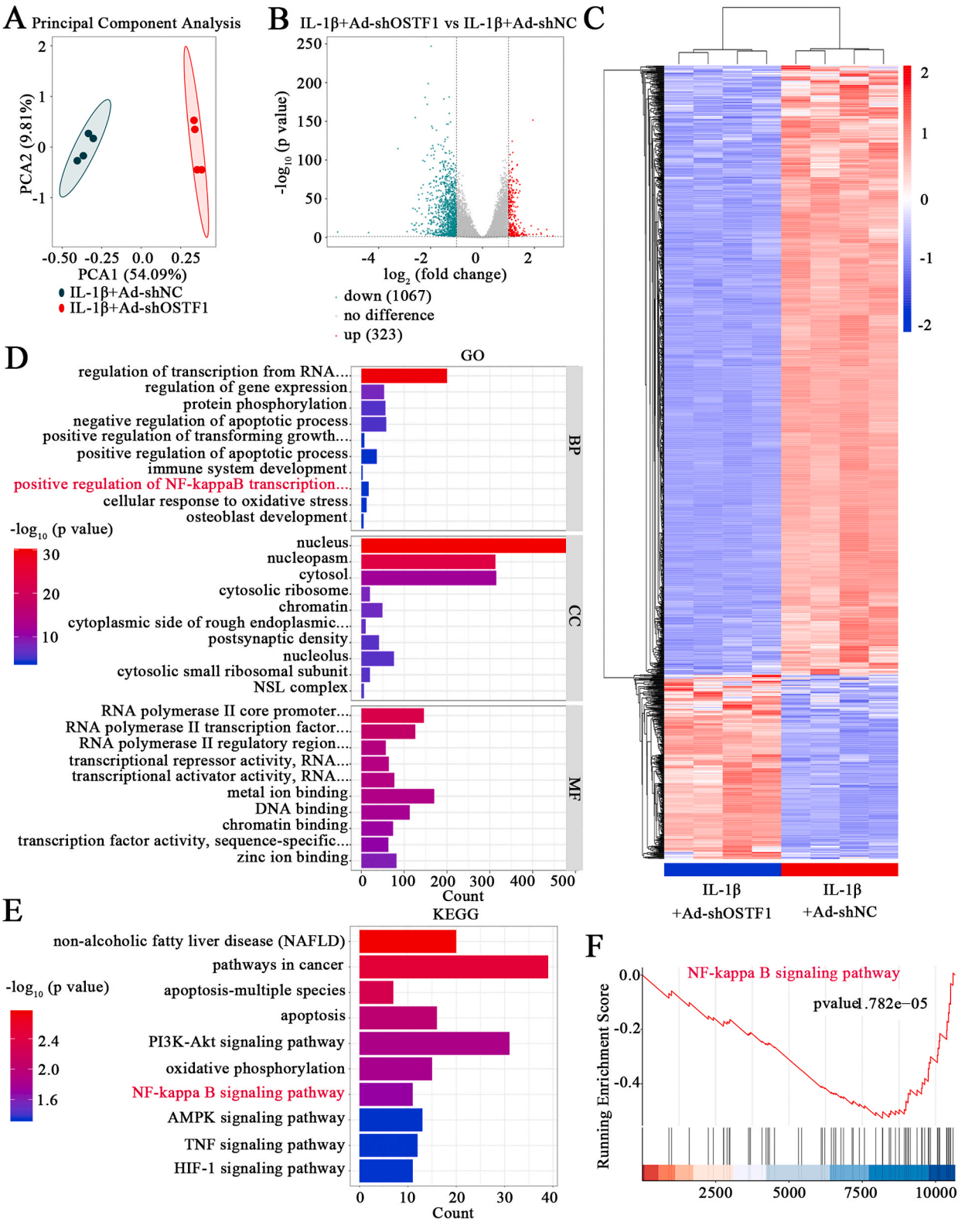

(caption on next page)

Fig. 6. Transcriptomic analysis of chondrocytes with IL-1β stimulation and OSTF1 knockdown. The rat chondrocytes were infected with adenovirus loaded with shOSTF1 or control and stimulated with IL-1β stimulation (10 ng/ml). Then the RNA sequencing was performed. IL-1β+Ad-shOSTF1 (n = 4) vs IL-1β+Ad-shNC (n = 4). (A) The principal component analysis. (B) The volcano plot showed the expression of DEGs. (C) The heatmap revealed the mRNA expression pattern of DEGs. (D–E) GO and KEGG enrichment analyzes. (F) GSEA analysis of DEGs enriched in the NF-κB signaling pathway.

3.5. OSTF1 knockdown inhibits IL-1β-induced the extracellular matrix degradation of chondrocytes

The degradation of articular cartilage may serve as a hallmark of OA pathogenesis. Therefore, we explored whether OSTF1 affects the cartilage matrix function. The levels of catabolic markers MMP1 and MMP13, as well as anabolic markers aggrecan and collagen-II were assessed in IL-1β-treated chondrocytes. Results of real time PCR and western blotting showed that OSTF1 knockdown markedly increased the levels of aggrecan and collagen-II, and decreased the levels of MMP1 and MMP13 (Fig. 5A–B). Altogether, OSTF1 knockdown inhibited the extracellular matrix degradation of chondrocytes induced by IL-1β, exhibiting the protective effects on chondrocytes.

3.6. Transcriptomic analysis of chondrocytes with IL-1β stimulation and OSTF1 knockdown

Rat chondrocytes were infected with adenovirus loaded with shOSTF1 or control and treated with IL-1β. Then we performed RNA sequencing analysis of the gene network regulated by OSTF1. Firstly, we used PCA to analyze the correlation between control samples and shOSTF1 samples and identified population differences. As shown in Fig. 6A, PCA data suggested that samples between groups were scattered and samples within groups were clustered together. Moreover, a volcano plot inferred the overall distribution of DEGs, of which 323 DEGs were upregulated and 1076 DEGs were downregulated (Fig. 6B). The heatmap revealed the mRNA expression levels of DEGs in chondrocytes (Fig. 6C). Additionally, we performed GO pathway analysis. DEGs were most involved in regulation of transcriptional from the RNA polymerase II promoter and negative regulation of apoptotic process in biological process, nucleus and cytosol in cellular component, and metal ion binding and RNA polymerase II core promoter proximal region sequence-specific DNA binding in molecular function, respectively (Fig. 6D). As observed, KEGG enrichment analysis showed that DEGs were significantly enriched in non-alcoholic fatty liver disease (NAFLD), pathways in cancer and apoptosis-multiple species (Fig. 6E). DEGs were also involved in NF-κB signaling pathway (Fig. 6D–E). Firstly, GSEA suggested the expression trend of DEGs in the NF-κB signaling pathway (Fig. 6F). These data revealed the gene network map of OSTF1, which may be valuable for subsequent screening important targets for OA.

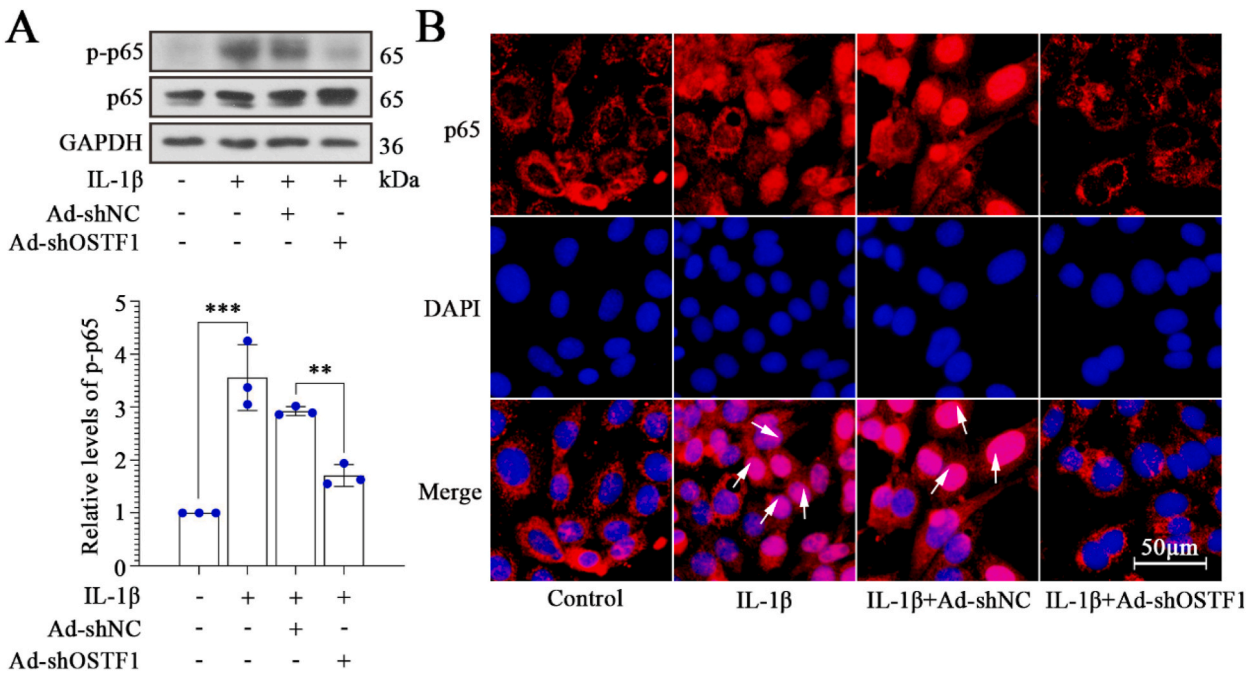

Fig. 7. OSTF1 knockdown inhibits the activation of NF-κB signaling pathway in chondrocytes. (A) Immunoblotting was used to detect the total and phosphorylation (Ser^{536}) levels of NF-κB p65. (B) Immunofluorescent staining exhibited the distribution of p65 in nuclei (the scale bar represented 50 μm, the arrows indicated the nuclear translocation of p65). n = 3. (**p < 0.01, ***p < 0.001).

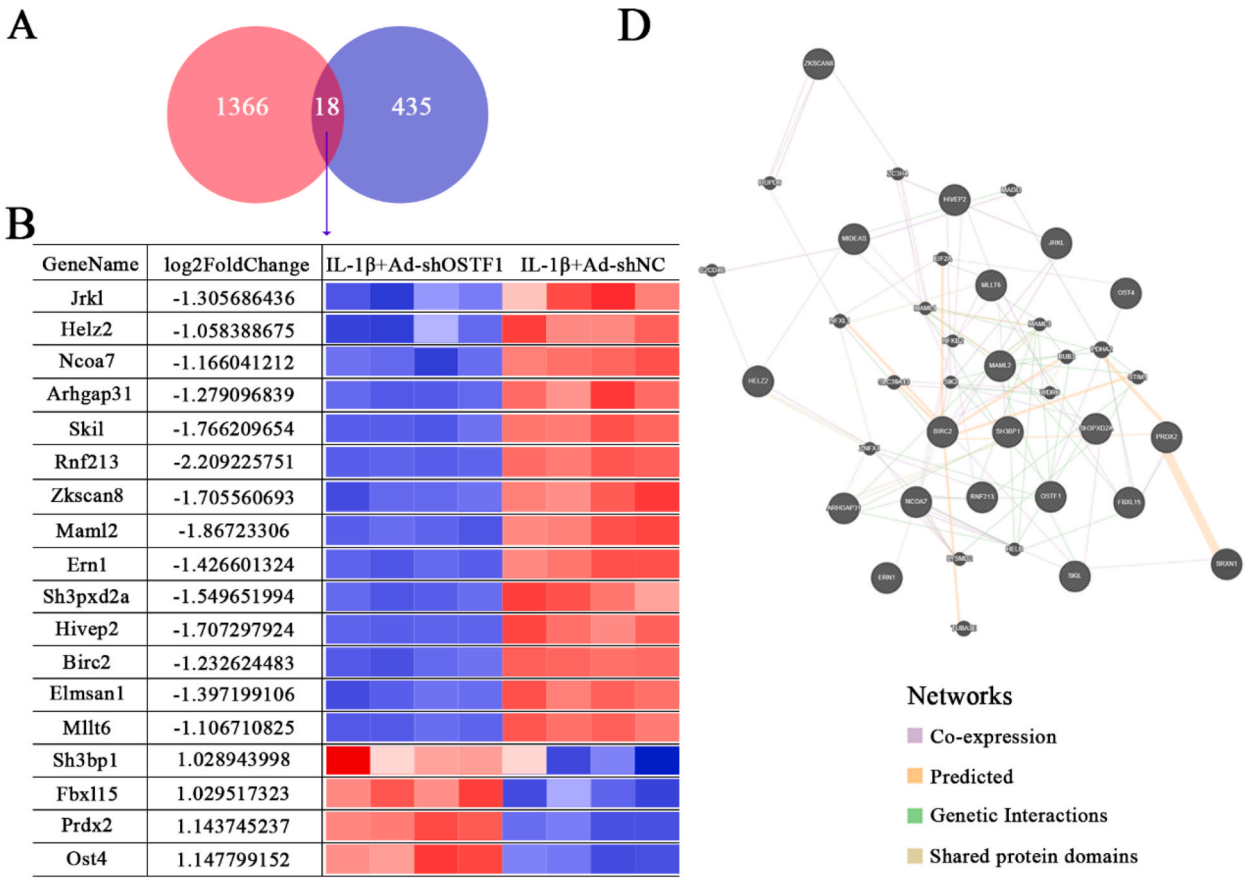

Fig. 8. Transcriptomic analysis reveals the potential gene network map regulated by OSTF1 and its downstream NF-κB. (A) The Venn diagram showed that 18 DEGs in OSTF1-silenced chondrocytes overlapped with NF-κB downstream targets predicted by hTFtarget database. (B) The heatmap revealed the mRNA expression pattern of these 18 DEGs. IL-1β+Ad-shOSTF1 (n = 4) vs IL-1β+Ad-shNC (n = 4). (C) The upset diagram revealed the correlation between these 18 DEGs and the total DEGs. (D) PPI analysis of OSTF1 and these 18 DEGs.

3.7. OSTF1 knockdown inhibits the activation of NF-κB signaling pathway in chondrocytes

The potential mechanism of OSTF1 was explored. Go and KEGG analyzes suggested that DEGs were involved in regulating NF-κB signaling pathway. NF-κB signaling pathway is related to the progression of OA and can induce chondrocyte apoptosis and inflammation [19]. Accordingly, we investigated the regulatory mechanism of OSTF1 on NF-κB signaling pathway. Western blotting analysis suggested that IL-1β increased the phosphorylation of p65, while OSTF1 knockdown decreased p-p65^{S536} levels (Fig. 7A). Notably, immunofluorescence staining presented that IL-1β stimulation promoted the nuclear translocation of p65, while OSTF1 knockdown significantly reduced nuclear translocation of p65, thereby inhibiting the activation of NF-κB signaling pathway (Fig. 7B). In short, these observations indicated that OSTF1 knockdown inhibited the NF-κB signaling activated by IL-1β.

Since our results reveal that OSTF1 knockdown inhibits the activation of NF-κB signaling pathway, we further analyzed the potential gene network map regulated by NF-κB, the downstream of OSTF1. The Venn diagram showed that 18 DEGs in OSTF1-silenced chondrocytes overlapped with the NF-κB downstream targets predicted by hTFtarget database (Fig. 8A). Hence, we then displayed the expression of 18 DEGs in chondrocytes by the heatmap (Fig. 8B). Among them, Jrkl, Helz2, Ncoa7, Arhgap31, Skil, Rnf213, Zkscan8, Maml2, Ern1, Sh3pxd2a, Hivep2, Birc2, Elmsan1 and Mllt6 were downregulated in OSTF1-silenced chondrocytes, while Sh3bp1, Fbxl15, Prdx2 and Ost4 were upregulated (Fig. 8B). Besides, the correlation between these 18 DEGs and the total DEGs was revealed by upset diagram, with a |correlation coefficient|>0.8 (Fig. 8C). Genemania database analysis showed the protein-protein interaction network between OSTF1 and these 18 DEGs (Fig. 8D). In the future, we may investigate the role of these 18 DEGs in OA.

4. Discussion

Firstly, in this study, we verified that OSTF1 expression was increased in the cartilage tissues of OA patients and OA rats. Next, we determined its potential roles during OA. As demonstrated, OSTF1 knockdown relieved the apoptosis, inflammation and extracellular matrix degradation, further suppressing IL-1β-mediated chondrocyte injury. The underlying mechanism of OSTF1 in OA was further explored. Our findings suggested that OSTF1 knockdown inactivated the NF-κB signaling pathway. In addition, we explored the potential gene network map regulated by OSTF1 and its downstream NF-κB. OSTF1 may be a novel target for treating OA.

OSTF1 was previously described as a cytoplasmic protein with SH3 and ankyrin domains [22]. It is also reported that OSTF1 is mainly expressed in osteoclasts and motor neurons [14]. In the present study, we found that the expression of OSTF1 was increased in cartilage tissues of OA patients. Notably, ACLT is one of the most common sports injuries [23]. The ACLT-induced OA model has been shown to reliably reproduce the various characteristics of human osteoarthritic bone for the study of OA [24]. In this study, we evaluated the damage of rat knee cartilage by a series of histological analyses in an ACLT-induced OA model and further investigated the expression of OSTF1 during OA. Our results showed that OSTF1 was upregulated in cartilage tissues of OA rats. Moreover, IL-1β is a cytokine that induces a series of pathogenic responses in chondrocytes and plays a crucial role in the process of OA [25,26]. Hence, IL-1β-treated chondrocytes were used as the cell model. In the current study, we discovered that IL-1β administration upregulated the expression levels of OSTF1 in rat chondrocytes.

Accumulating evidence has suggested that OSTF1 participates in the formation of osteoclasts, indirectly activates osteoclast differentiation and regulates the activity of bone-resorbing [27,28]. Recently, a study has shown that OSTF1 plays a vital role in bone development [14]. In this work, we silenced the expression of OSTF1 to explore the role of OSTF1 knockdown on IL-1β-induced chondrocyte injury. Our findings investigated that OSTF1 knockdown largely increased the chondrocyte viability inhibited by IL-1β, which implied that OSTF1 may exert protective effects on chondrocytes.

Previous studies have reported that apoptosis is important in many biological processes [29–31]. Caspase-3 is the major executor of apoptosis [32]. One of the basic substrates cleaved by caspase-3 is poly ADP-ribose polymerase (PARP), an abundant DNA-binding enzyme that detects and signals DNA strand breaks [33]. The presence of cleaved PARP is one of the most commonly used diagnostic tools to determine apoptosis in many cell types [34]. Therefore, the upregulation of cleaved Caspase-3 and cleaved PARP may be considered as important symbols in the progression of apoptosis. Importantly, the present study identified that OSTF1 knockdown relieved IL-1β-induced apoptosis, as reflected by decreased TUNEL-positive chondrocytes, as well as the levels of cleaved caspase-3 and cleaved PARP. Thus, our data revealed that OSTF1 knockdown not only increased chondrocytes viability but also inhibited apoptosis during OA, therefore protecting chondrocytes from damage induced by IL-1β treatment.

The inflammatory responses are associated with the development of OA. Elevated levels of pro-inflammatory cytokines such as IL-1β and TNF-α are often observed in OA patients [35]. The proinflammatory cytokines IL-1β, IL-6 and TNF-α can stimulate chondrocytes and promote metabolic imbalance, resulting in the pathological development of OA [36]. Herein, our findings indicated that OSTF1 knockdown downregulated the levels of IL-6 and TNF-α elevated by IL-1β, showing anti-inflammatory effects. OA is also characterized by a senescence-associated secretory phenotype and matrix degradation leading to a gradual loss of articular cartilage integrity [37]. In this study, we evaluated the levels of extracellular proteolytic enzymes associated with cartilage degradation, and our results suggested that OSTF1 knockdown inhibited the levels of catabolic markers MMP1 and MMP13 and increased the levels of anabolic markers aggrecan and collagen-II. These observations confirmed that OSTF1 knockdown had the protective effects on chondrocytes.

Recently, single-cell RNA-seq analysis has revealed the progression of human OA and further identified chondrocyte biomarkers [38,39]. In our study, transcriptomic analysis was utilized to explore the gene network map regulated by OSTF1. In this work, a volcano plot displayed the overall distribution of DEGs, and a heatmap revealed the mRNA expression pattern of DEGs in chondrocytes. Additionally, we performed GO and KEGG pathway analyzes. DEGs were most involved in regulation of transcriptional from the RNA polymerase II promoter and negative regulation of apoptotic process in biological process, nucleus and cytosol in cellular component, and metal ion binding and RNA polymerase II core promoter proximal region sequence-specific DNA binding in molecular

function, respectively. KEGG enrichment analysis showed that DEGs were significantly enriched in NAFLD, pathways in cancer and apoptosis-multiple species. Also, these DEGs were enriched in NF-κB signaling pathway. These results revealed the gene network map regulated by OSTF1.

The underlying mechanism of OSTF1 was then explored. Transcriptomic analysis indicated that DEGs participated in regulating NF-κB signaling pathway. Herein, we investigated the regulatory mechanism of OSTF1 on NF-κB signaling pathway. NF-κB is the main representative transcription factor activated by cellular stimulation with IL-1β [40,41]. NF-κB pathway is a prototypical proinflammatory signaling pathway, which may lead to the apoptosis or damage of chondrocytes [40]. In addition, increasing evidence has indicated that the phosphorylation of p65 can reflect the activation of NF-κB, and Ser536 is an important phosphorylation site of p65 [42]. The present study verified that OSTF1 knockdown inhibited the activation of NF-κB signaling pathway. To our best knowledge, NF-κB signaling pathway is regulated by OSTF1 is novel.

Since our results reveal that OSTF1 knockdown inhibits the NF-κB signal, we further analyzed the potential gene network map regulated by NF-κB, the downstream of OSTF1. Our results showed that 18 DEGs in OSTF1-silenced chondrocytes overlapped with the NF-κB downstream targets. The upset diagram presented the correlation between these 18 DEGs and the total DEGs. PPI showed the protein-protein interaction network between OSTF1 and these 18 DEGs. In the future, we will conduct more in-depth studies on these 18 DEGs. Based on the above findings, the results of transcriptomic analysis may serve as a theoretical basis for screening more valuable targets for OA.

There were several limitations in this study. First, the clinical results need to be further confirmed by expanding the sample. In this work, we used an IL-1β-induced chondrocyte model *in vitro* to investigate the role of OSTF1. In addition, the primary chondrocytes obtained from a rat model of OA will also help to better represent the complex pathogenesis of OA. In future studies, primary chondrocytes obtained from the OA rat model may be employed to better understand the role of OSTF1 during OA. Many studies have shown that PI3K/AKT/mTOR and TGF-β1 signaling pathways are associated with the progression of OA [43–45]. Whether other signaling pathways, such as AKT and TGF-β1, are involved in the OSTF1-affected OA process will also be further explored. In addition, our study confirmed that OSTF1 knockdown inhibited the NF-κB signaling pathway. Because IL-1β caused the activation of NF-κB signaling pathway in chondrocytes, which may act as an activator of NF-κB, we did not use the activator of NF-κB for the recovery experiment.

Our study is the first to find that OSTF1 knockdown alleviates OA through suppressing the NF-κB signaling pathway (Fig. 9). In addition, we reveal the gene network map regulated by OSTF1 and its downstream NF-κB in chondrocytes. Our study provides novel insights into the function and mechanism of OSTF1 during OA.

Funding

This research did not receive any specific grant from funding agencies in the public, commercial, or not-for-profit sectors.

Data availability statement

Data are available upon reasonable request.

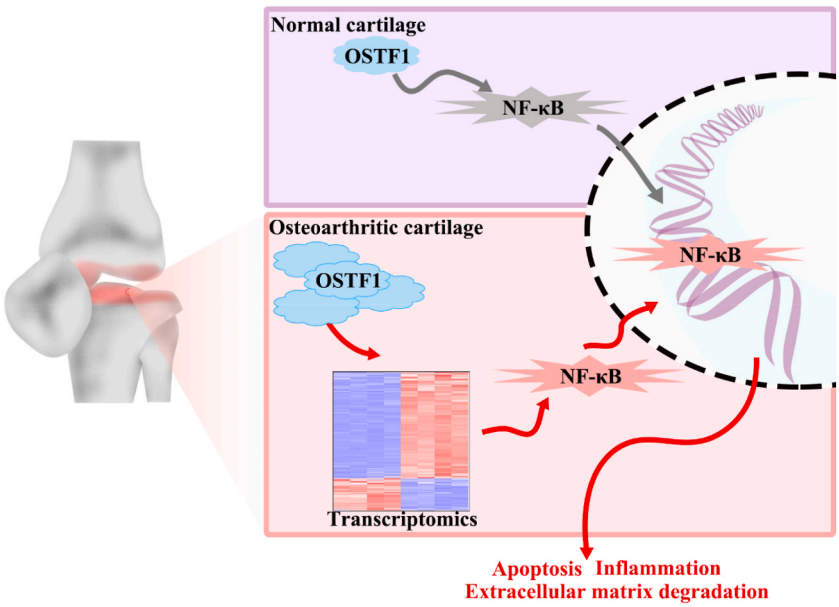

Fig. 9. The diagram showed the role and the underlying mechanism of OSTF1 during OA.

Ethics statement

Ethical approval was obtained from the Medical Research Ethics Committee of the First Affiliated Hospital of Anhui Medical University (Quick-PJ 2022-03-36), and clinical study was conducted in accordance with the Declaration of Helsinki. Animal experiments were approved by the Medical Research Ethics Committee of Anhui Medical University (LISC 20221035) and carried out in accordance with the "Guide for the Care and Use of Laboratory Animals".

CRediT authorship contribution statement

Bin Hu: Writing – original draft, Methodology, Formal analysis, Data curation. **Gongwen Du:** Writing – review & editing, Visualization, Conceptualization.

Declaration of competing interest

The authors declare that they have no known competing financial interests or personal relationships that could have appeared to influence the work reported in this paper.

Appendix A. Supplementary data

Supplementary data to this article can be found online at https://doi.org/10.1016/j.heliyon.2024.e30110.

References

[1] S. Krasnokutsky, J. Samuels, S.B. Abramson, Osteoarthritis in 2007, Bull NYU Hosp Jt Dis 65 (2007) 222–228.
[2] B. Xia, C. Di, J. Zhang, S. Hu, H. Jin, P. Tong, Osteoarthritis pathogenesis: a review of molecular mechanisms, Calcif. Tissue Int. 95 (2014) 495–505.
[3] D.J. Hunter, S. Bierma-Zeinstra, Osteoarthritis, Lancet 393 (2019) 1745–1759.
[4] D.T. Felson, Clinical practice. Osteoarthritis of the knee, N. Engl. J. Med. 354 (2006) 841–848.
[5] M.B. Goldring, S.R. Goldring, Osteoarthritis, J. Cell. Physiol. 213 (2007) 626–634.
[6] W.H. Ettinger Jr., R. Burns, S.P. Messier, W. Applegate, W.J. Rejeski, T. Morgan, S. Shumaker, M.J. Berry, M. O'Toole, J. Monu, T. Craven, A randomized trial comparing aerobic exercise and resistance exercise with a health education program in older adults with knee osteoarthritis. The Fitness Arthritis and Seniors Trial (FAST), JAMA 277 (1997) 25–31.
[7] S.P. Messier, R.F. Loeser, G.D. Miller, T.M. Morgan, W.J. Rejeski, M.A. Sevick, W.H. Ettinger Jr., M. Pahor, J.D. Williamson, Exercise and dietary weight loss in overweight and obese older adults with knee osteoarthritis: the Arthritis, Diet, and Activity Promotion Trial, Arthritis Rheum. 50 (2004) 1501–1510.
[8] B.M. Berman, L. Lao, P. Langenberg, W.L. Lee, A.M. Gilpin, M.C. Hochberg, Effectiveness of acupuncture as adjunctive therapy in osteoarthritis of the knee: a randomized, controlled trial, Ann. Intern. Med. 141 (2004) 901–910.
[9] S.S. Leopold, Minimally invasive total knee arthroplasty for osteoarthritis, N. Engl. J. Med. 360 (2009) 1749–1758.
[10] A. Jackson, W. Gu, Transport properties of cartilaginous tissues, Curr. Rheumatol. Rev. 5 (2009) 40.
[11] M.B. Goldring, K.B. Marcu, Cartilage homeostasis in health and rheumatic diseases, Arthritis Res. Ther. 11 (2009) 224.
[12] J.P. Pelletier, J. Martel-Pelletier, S.B. Abramson, Osteoarthritis, an inflammatory disease: potential implication for the selection of new therapeutic targets, Arthritis Rheum. 44 (2001) 1237–1247.
[13] J.S. Mort, C.J. Billington, Articular cartilage and changes in arthritis: matrix degradation, Arthritis Res. 3 (2001) 337–341.
[14] M. Vermeren, R. Lyraki, S. Wani, R. Airik, O. Albagha, R. Mort, F. Hildebrandt, T. Hurd, Osteoclast stimulation factor 1 (Ostf1) KNOCKOUT increases trabecular bone mass in mice, Mamm. Genome 28 (2017) 498–514.
[15] L. Chen, Y. Wang, D. Wells, D. Toh, H. Harold, J. Zhou, E. DiGiammarino, E.J. Meehan, Structure of the SH3 domain of human osteoclast-stimulating factor at atomic resolution, Acta Crystallogr., Sect. F: Struct. Biol. Cryst. Commun. 62 (2006) 844–848.
[16] J.P. Caron, J.C. Fernandes, J. Martel-Pelletier, G. Tardif, F. Mineau, C. Geng, J.P. Pelletier, Chondroprotective effect of intraarticular injections of interleukin-1 receptor antagonist in experimental osteoarthritis. Suppression of collagenase-1 expression, Arthritis Rheum. 39 (1996) 1535–1544.
[17] F.A. van de Loo, L.A. Joosten, P.L. van Lent, O.J. Arntz, W.B. van den Berg, Role of interleukin-1, tumor necrosis factor alpha, and interleukin-6 in cartilage proteoglycan metabolism and destruction. Effect of in situ blocking in murine antigen- and zymosan-induced arthritis, Arthritis Rheum. 38 (1995) 164–172.
[18] K.B. Marcu, M. Otero, E. Olivotto, R.M. Borzi, M.B. Goldring, NF-kappaB signaling: multiple angles to target OA, Curr. Drug Targets 11 (2010) 599–613.
[19] D. Gun Bilgic, O.F. Hatipoglu, S. Cigdem, A. Bilgic, T. Cora, NF-kbeta upregulates ADAMTS5 expression by direct binding after TNF-alpha treatment in OUMS-27 chondrosarcoma cell line, Mol. Biol. Rep. 47 (2020) 4215–4223.
[20] D. Nemirov, Y. Nakagawa, Z. Sun, A. Lebaschi, S. Wada, C. Carballo, X.H. Deng, D. Putnam, L.J. Bonassar, S.A. Rodeo, Effect of lubricin mimetics on the inhibition of osteoarthritis in a rat anterior cruciate ligament transection model, Am. J. Sports Med. 48 (2020) 624–634.
[21] H. Xue, Y. Tu, T. Ma, T. Wen, T. Yang, L. Xue, M. Cai, F. Wang, M. Guan, miR-93-5p attenuates IL-1beta-induced chondrocyte apoptosis and cartilage degradation in osteoarthritis partially by targeting TCF4, Bone 123 (2019) 129–136.
[22] S. Nakamura, R. Masuyama, K. Sakai, K. Fukuda, K. Takeda, S. Tanimura, SH3P2 suppresses osteoclast differentiation through restricting membrane localization of myosin 1E, Gene Cell. 25 (2020) 707–717.
[23] N. Aizah, P.P. Chong, T. Kamarul, Early alterations of subchondral bone in the rat anterior cruciate ligament transection model of osteoarthritis, Cartilage 13 (2021) 1322S–1333S.
[24] C. Zhao, Q. Liu, K. Wang, Artesunate attenuates ACLT-induced osteoarthritis by suppressing osteoclastogenesis and aberrant angiogenesis, Biomed. Pharmacother. 96 (2017) 410–416.
[25] F. Morrovati, N. Karimian Fathi, J. Soleimani Rad, A. Montaseri, Mummy prevents IL-1beta-induced inflammatory responses and cartilage matrix degradation via inhibition of NF-B subunits gene expression in pellet culture system, Adv. Pharmaceut. Bull. 8 (2018) 283–289.
[26] T. Pan, R. Chen, D. Wu, N. Cai, X. Shi, B. Li, J. Pan, Alpha-Mangostin suppresses interleukin-1beta-induced apoptosis in rat chondrocytes by inhibiting the NF-kappaB signaling pathway and delays the progression of osteoarthritis in a rat model, Int. Immunopharm. 52 (2017) 156–162.
[27] S. Tong, H. Zhou, Y. Gao, Z. Zhu, X. Zhang, M. Teng, L. Niu, Crystal structure of human osteoclast stimulating factor, Proteins 75 (2009) 245–251.
[28] S. Reddy, R. Devlin, C. Menaa, R. Nishimura, S.J. Choi, M. Dallas, T. Yoneda, G.D. Roodman, Isolation and characterization of a cDNA clone encoding a novel peptide (OSF) that enhances osteoclast formation and bone resorption, J. Cell. Physiol. 177 (1998) 636–645.

[29] A.H. Wyllie, Apoptosis and the regulation of cell numbers in normal and neoplastic tissues: an overview, Cancer Metastasis Rev. 11 (1992) 95–103.
[30] G. Pistritto, D. Trisciuoglio, C. Ceci, A. Garufi, G. D'Orazi, Apoptosis as anticancer mechanism: function and dysfunction of its modulators and targeted therapeutic strategies, Aging (Albany NY) 8 (2016) 603–619.
[31] X. Xu, Y. Lai, Z.C. Hua, Apoptosis and apoptotic body: disease message and therapeutic target potentials, Biosci. Rep. 39 (2019).
[32] A.M. Gown, M.C. Willingham, Improved detection of apoptotic cells in archival paraffin sections: immunohistochemistry using antibodies to cleaved caspase 3, J. Histochem. Cytochem. 50 (2002) 449–454.
[33] P. Decker, S. Muller, Modulating poly (ADP-ribose) polymerase activity: potential for the prevention and therapy of pathogenic situations involving DNA damage and oxidative stress, Curr. Pharmaceut. Biotechnol. 3 (2002) 275–283.
[34] D.W. Koh, T.M. Dawson, V.L. Dawson, Mediation of cell death by poly(ADP-ribose) polymerase-1, Pharmacol. Res. 52 (2005) 5–14.
[35] S. Min, C. Wang, W. Lu, Z. Xu, D. Shi, D. Chen, H. Teng, Q. Jiang, Serum levels of the bone turnover markers dickkopf-1, osteoprotegerin, and TNF-alpha in knee osteoarthritis patients, Clin. Rheumatol. 36 (2017) 2351–2358.
[36] A.V. Miagkov, D.V. Kovalenko, C.E. Brown, J.R. Didsbury, J.P. Cogswell, S.A. Stimpson, A.S. Baldwin, S.S. Makarov, NF-kappaB activation provides the potential link between inflammation and hyperplasia in the arthritic joint, Proc. Natl. Acad. Sci. U. S. A. 95 (1998) 13859–13864.
[37] Y. He, Q. Ding, W. Chen, C. Lin, L. Ge, C. Ying, K. Xu, Z. Wu, L. Xu, J. Ran, W. Chen, L. Wu, LONP1 downregulation with ageing contributes to osteoarthritis via mitochondrial dysfunction, Free Radic. Biol. Med. 191 (2022) 176–190.
[38] Q. Ji, Y. Zheng, G. Zhang, Y. Hu, X. Fan, Y. Hou, L. Wen, L. Li, Y. Xu, Y. Wang, F. Tang, Single-cell RNA-seq analysis reveals the progression of human osteoarthritis, Ann. Rheum. Dis. 78 (2019) 100–110.
[39] X. Zhang, N. Huang, R. Huang, L. Wang, Q. Ke, L. Cai, S. Wu, Single-cell rna seq analysis identifies the biomarkers and differentiation of chondrocyte in human osteoarthritis, Am J Transl Res 12 (2020) 7326–7339.
[40] T. Lawrence, The nuclear factor NF-kappaB pathway in inflammation, Cold Spring Harbor Perspect. Biol. 1 (2009) a001651.
[41] A. Oeckinghaus, S. Ghosh, The NF-kappaB family of transcription factors and its regulation, Cold Spring Harbor Perspect. Biol. 1 (2009) a000034.
[42] T. Valovka, M.O. Hottiger, p65 controls NF-kappaB activity by regulating cellular localization of IkappaBbeta, Biochem. J. 434 (2011) 253–263.
[43] X. Zhou, J. Li, Y. Zhou, Z. Yang, H. Yang, D. Li, J. Zhang, Y. Zhang, N. Xu, Y. Huang, L. Jiang, Down-regulated ciRS-7/up-regulated miR-7 axis aggravated cartilage degradation and autophagy defection by PI3K/AKT/mTOR activation mediated by IL-17A in osteoarthritis, Aging (Albany NY) 12 (2020) 20163–20183.
[44] J. Li, M. Jiang, C. Xiong, J. Pan, S. Jia, Y. Zhang, J. Zhang, N. Xu, X. Zhou, Y. Huang, KLF4, negatively regulated by miR-7, suppresses osteoarthritis development via activating TGF-beta1 signaling, Int. Immunopharm. 102 (2022) 108416.
[45] J. Li, M. Jiang, Z. Yu, C. Xiong, J. Pan, Z. Cai, N. Xu, X. Zhou, Y. Huang, Z. Yang, Artemisinin relieves osteoarthritis by activating mitochondrial autophagy through reducing TNFSF11 expression and inhibiting PI3K/AKT/mTOR signaling in cartilage, Cell. Mol. Biol. Lett. 27 (2022) 62.